Journal of Organometallic Chemistry, 214 (1981) 233—252
Elsevier Sequoia S.A., Lausanne — Printed in The Netherlands

THE ACTIVATION OF CARBON DISULFIDE BY BINUCLEAR RHODIUM COMPLEXES AND THE STRUCTURE OF $[Rh_2Cl_2(CO)(C_2S_4)(Ph_2PCH_2PPh_2)_2]$

MARTIN COWIE * and STEPHEN K. DWIGHT

Department of Chemistry, The University of Alberta, Edmonton, Alberta T6G 2G2 (Canada)

(Received September 22nd, 1980)

Summary

The reactions of *trans*-$[RhCl(CO)(DPM)]_2$ (1) (DPM = $Ph_2PCH_2PPh_2$) and $[Rh_2Cl_2(\mu\text{-}CO)(DPM)_2]$ (2) with CS_2 have been investigated and the final product of each reaction, $[Rh_2Cl_2(CO)(C_2S_4)(DPM)_2]$ (3), has been structurally characterized by X-ray crystallography. A scheme for the reaction of 2 is presented based on monitoring the stepwise addition of CS_2 using $^{31}P\{^1H\}$ and $^{13}C\{^{31}P\{^1H\}\}$ NMR and infrared spectroscopy. The scheme for the reaction of 1 is based on infrared and $^{31}P\{^1H\}$ NMR data and on analogies with the reaction of 2, and with the similar, well characterized reactions of 1 with SO_2. Compound 3 crystallizes in the space group $P2_1/c$ with a = 22.311(3) Å, b = 22.843(3) Å, c = 22.828(3) Å, β = 115.21(1)° and Z = 8. Based on 5929 observed reflections the structure was refined to R = 0.112 and R_w = 0.143 based on group refinement for the phenyl rings and isotropic refinement for all other non-hydrogen atoms. Slight differences in the geometries of the two independent dimers are observed resulting from different DPM phenyl ring orientations. However, the major features of the two dimers are the same, having a C_2S_4 fragment bridging two quasi-octahedral rhodium atoms and bound by a sulfur (Rh—S (dimers A&B) = 2.347(7), 2.356(7) Å) and a carbon atom (Rh—C = 1.90(2), 1.95(2) Å) to one rhodium center and by a sulfur atom (Rh—S = 2.386(7), 2.393(7) Å) to the other rhodium center. Other relevant parameters are: Rh(1)—Rh(2) = 2.811(3), 2.810(3) Å; Rh(1)—Cl(1) = 2.428(6), 2.455(6) Å; Rh(2)—Cl(2) = 2.508(8), 2.527(8) Å; Rh(2)—C(1)O(1) = 1.87(2), 1.96(3) Å.

Introduction

Much of the recent interest in carbon disulfide chemistry stems from the close similarity of this molecule to the less reactive carbon dioxide molecule.

Although CS_2 chemistry has been actively pursued since the mid 60's [1] few complexes containing this molecule have been structurally characterized [2—9] and even fewer structures of CO_2 complexes are known [10—12]. For the more extensively studied CS_2 molecule the commonest coordination mode, and one of the bonding modes also observed for the analogous CO_2 molecule [10], has the CS_2 molecule bound to the metal in a side-on manner through the carbon atom and one of the sulfur atoms [2,5—8] (the C,S-η^2 mode).

Although several CS_2 complexes of rhodium and iridium have been prepared [13,14], none had been structurally characterized until recently [9]. In several of these complexes the C,S-η^2 bonding mode of the CS_2 molecule had been inferred based on analogies with other structurally characterized transition metal complexes [13,14], even though the C—S stretching frequencies observed were typically ca. 100 cm^{-1} lower than those observed in the structurally confirmed complexes. These low values of ν(CS) suggest that the CS_2 molecule may adopt another coordination geometry in these rhodium and iridium complexes. One possibility which must be considered involves the condensation of the CS_2 molecules. Rhodium has previously displayed a tendency of condensing sulfur-containing ligands. For example, in $[RhCl(PPh_3)_2(PhCONCS)_2]$ [15] and $[RhCl(PPh_3)_2(C_2H_5OCONCS)_3]$ [16] two molecules of PhCONCS and three molecules of $C_2H_5OCONCS$, respectively, are condensed at the metal centers. Significantly, one of the few structurally characterized CO_2 complexes actually contains a C_2O_4 fragment resulting from the condensation of two CO_2 molecules at an iridium center [11]. The CO stretching frequencies for this species are 25—75 cm^{-1} lower than those in a typical C,O-η^2-bound species [10]. Furthermore, while this work was in progress the structural determination of $[Rh(C_2S_4)(\eta^5\text{-}C_5H_5)(PMe_3)]$ [9] was reported and indicated that the C_2S_4 fragment was bound in an analogous manner to the above C_2O_4 moiety and again the values of ν(CS) for this species were low.

In view of the obvious lack of structural information available on rhodium CS_2 complexes, the present study was undertaken in order to form a much-needed basis for spectral and structural correlations in these complexes and to gain a better understanding of transition metal activation of CS_2 and related molecules.

Experimental

All reactions were performed under a dinitrogen atmosphere using degassed solvents. Infrared spectra were recorded on a Perkin-Elmer Model 467 spectrometer using Nujol mulls on KBr plates unless otherwise specified. $^{31}P\{^1H\}$ and $^{13}C\{^{31}P\{^1H\}\}$ NMR spectra were recorded on a Bruker HFX-90 spectrometer.

Preparation of $[Rh_2Cl_2(CO)(C_2S_4)(DPM)_2]$

A suspension of 0.200 g (0.182 mmol) of *trans*-$[RhCl(CO)(DPM)]_2$ (1) * in 25 ml of CH_2Cl_2 was treated with 10 ml of CS_2 and allowed to react for 24 h. To the resulting red solution was added 25 ml of diethyl ether to induce crys-

* DPM = $Ph_2PCH_2PPh_2$.

tallization. The red microcrystalline sample of 3, obtained in about 80% yield, showed the following bands in the infrared spectrum: ν(CO) = 2040(sh), 2020s cm^{-1}; ν(CS) = 1050m, 995(sh), 980s cm^{-1}. Although satisfactory elemental analyses were obtained for C, H and Cl, suitable results for S were never obtained. Elemental analyses: Found: C, 51.6; H, 4.56; Cl, 6.23; S, 4.11. $[Rh_2Cl_2(CO)(C_2S_4)(DPM)_2]$, calcd.: C, 51.9; H, 3.61; Cl, 5.78; S, 10.5%. Compound 3 was also prepared in a manner analogous to that shown above, from the reaction of CS_2 with a CH_2Cl_2 solution of $[Rh_2Cl_2(\mu\text{-}CO)(DPM)_2]$.

Spectroscopic studies

A solution was prepared by dissolving 0.100 g (0.072 mmol) of $[Rh_2Cl_2(\mu\text{-}CO)(DPM)_2]$ (2) in 4 ml of CD_2Cl_2 in a 10 mm NMR tube. The $^{31}P\{^1H\}$ NMR spectrum was recorded at 233 K. Subsequent $^{31}P\{^1H\}$ NMR spectra were then recorded after each 1.5 μl (0.025 mmol) addition of CS_2 until all of 2 had been converted to $[Rh_2Cl_2(CO)(C_2S_4)(DPM)_2]$ (3). In addition to resonances assignable to 2 (δ = 19.7 ppm *; $|^1J(Rh—P) + {}^xJ(Rh—P)|$** = 115.9 Hz) and 3 ($\delta$ = 7.5 ppm; AA'BB'XY multiplet), two additional resonances due to symmetric species at δ = 15.7 ppm ($|^1J(Rh—P) + {}^xJ(Rh—P)|$ = 116.5 Hz) and δ = 14.3 ppm ($|^1J(Rh—P) + {}^xJ(Rh—P)|$ = 98.2 Hz) were also observed at intermediate times in the reaction. The $^{13}C\{^{31}P\{^1H\}\}$ NMR spectra were similarly monitored using exactly the same technique and starting with $[Rh_2Cl_2(\mu\text{-}^{13}CO)(DPM)_2]$. Carbonyl resonances assignable to 2 (δ = 229.0 ppm ***; triplet; $|J(Rh—C)|$ = 44.9 Hz), 3 (δ = 191.5 ppm; doublet; $|J(Rh—C)|$ = 69.1 Hz) and a third species (δ = 186.5 ppm; doublet; $|J(Rh—C)|$ = 80.1 Hz) were observed.

Infrared spectra were obtained in an analogous manner, by recording the solution spectrum after each stepwise addition of 7 μl (0.116 mmol) of CS_2 to a CH_2Cl_2 solution of 2 (0.500 g, 0.465 mmol, in 30 ml). Unfortunately, the CS_2 stretching region was obscured by DPM and free CS_2 bands. In the bridging carbonyl region only one band, attributable to 2, was observed (ν(CO) = 1750 cm^{-1}). In addition, two vibrations were observed in the terminal carbonyl region; the one at 2030 cm^{-1} increased in intensity throughout the experiment and was assigned to species 3, and the second at 1990 cm^{-1} was observed at intermediate times in the experiment.

Crystallization of $[Rh_2Cl_2(CO)(C_2S_4)(DPM)_2]$

To a solution of 0.100 g (0.0798 mmol) of 3 in 10 ml of CH_2Cl_2 were added 2 ml of CS_2 and 7 ml of diethyl ether. Crystallization was induced from this solution by slow cooling, yielding red crystals. An infrared spectrum verified that it was species 3.

X-Ray data collection

Red crystals of $[Rh_2Cl_2(CO)(C_2S_4)(DPM)_2]$ were mounted in glass capillaries. Preliminary film data showed that these crystals were of only mediocre quality;

---

* Positive δ values are downfield from H_3PO_4.

** $|^1J(Rh—P) + {}^xJ(Rh—P)|$ is taken as the splitting between the two major peaks.

*** Positive δ values are downfield from external tetramethylsilane (TMS).

however, repeated attempts to obtain crystals of better quality failed. The structural investigation was therefore continued on the original crystals. These crystals belong to the monoclinic system with extinctions ($h0l$, l odd; $0k0$, k odd) characteristic of the centrosymmetric space group $P2_1/c$. The density calculation, and the cell parameters, indicated that $Z = 8$, revealing that two independent dimers per asymmetric unit were present. Therefore, a cell reduction [17] was performed to rule out the possibility that the crystals might belong to a system of higher symmetry. The cell reduction confirmed the $P2_1/c$ cell as the reduced cell and the solution of the structure verified this, showing that the two independent dimers in the asymmetric unit have slight but significant differences in their geometries (vide infra) and different orientations.

Accurate cell parameters were obtained by a least-squares analysis of the setting angles of 12 carefully centered reflections chosen from diverse regions of reciprocal space ($50° < 2\theta < 70°$, Cu-K_α radiation) and obtained by using a

TABLE 1

SUMMARY OF CRYSTAL DATA AND INTENSITY COLLECTION FOR $[Rh_2Cl_2(CO)(C_2S_4)(DPM)_2]$

Compound	$[Rh_2Cl_2(CO)(C_2S_4)(DPM)_2]$
Formula	$C_{53}H_{44}Cl_2O_2P_4Rh_2S_4$
Formular weight	1225.80
Cell parameters	
a (Å)	22.311(3)
b (Å)	22.843(3)
c (Å)	22.828(3)
β (°)	115.21(1)
V (Å^3)	10526
Z	8
Density (g cm^{-3})	1.547 (calcd.) 1.56(2) (expt'l. by flotation)
Space group	C_{2h}^5—$P2_1/c$
Crystal dimensions (mm)	0.586 X 0.211 X 0.629
Crystal volume (mm^3)	0.0458 mm^3
Crystal faces	Of the form {100}, {101}, and {010}
Temperature (°C)	20
Radiation	Cu-K_α (λ = 1.540562 Å) filtered with 0.5 mm thick nickel foil
μ (cm^{-1})	90.85
Range in absorption correction factors	0.081—0.230
Receiving aperture (mm)	6 X 6; 30 cm from the crystal
Takeoff angle (°)	6.2°
Scan speed	2° in 2θ/min
Scan range (°)	1.00 below $K_{\alpha 1}$ to 1.00 above $K_{\alpha 2}$
Background counting time (s)	10 ($2° \leq 2\theta \leq 80°$) 20 ($80° < 2\theta \leq 100°$)
2θ limits (°)	$2 \leq 2\theta \leq 100$
2θ limits for centered reflections (°)	$50 \leq 2\theta \leq 60$
Final number of variables	337
Unique data collected	11195
Unique data used ($F_0^2 \geq 3\sigma(F_0^2)$)	5929
Error in observation of unit weight	2.467
R	0.112
R_w	0.143

narrow X-ray source (see Table 1 for pertinent crystal data).

Intensity data were collected on a Picker four-circle automated diffractometer equipped with a scintillation counter and pulse-height analyzer tuned to accept 90% of the Cu-K_α peak. Background counts were measured at both ends of the scan range with crystal and counter stationary. Standard deviations in the intensities were computed using a value of 0.05 for p [18]. The intensities of three standard reflections were measured automatically every 100 reflections and four additional standards were measured three times a day. All standards underwent an approximate 10% linear decay and the data were corrected for this apparent decomposition.

The intensities of 11195 unique reflections were measured using Cu-K_α radiation between the limits $3° \leqslant 2\theta \leqslant 100°$. Data collection was suspended at $2\theta = 100°$ since beyond this few reflections were observed. Of the measured reflections only 5929 were significantly above background ($F^2/\sigma(F^2) \geqslant 3.0$) and were used in subsequent calculations. During data collection a clear colourless liquid was observed condensing on the inside of the capillary. However, by the time data collection had finished this liquid had disappeared (presumably though a pinhole in the capillary) so no identification of this liquid was possible. Absorption corrections were applied to the data using Gaussian integration [19].

Solution of structure

The Rh and P atom positions were derived using a combination of Patterson syntheses and direct methods (Multan [20]). Solution of the structure was not trivial owing to the orientations of the two independent dimers which had the Rh—P vectors of one dimer parallel to the Rh—Rh vector of the other. The remaining atoms were located from subsequent least-squares calculations and electron density difference maps. Structure factors were calculated using the atomic scattering factors taken from Cromer and Waber's tabulation [21] for all atoms except hydrogen for which the values of Stewart et al. [22] were used. Anomalous dispersion terms [23] for Rh, P, Cl and S were included in F_c. The phenyl carbon atoms were refined as rigid groups and hydrogen atoms, although located, were included in their idealized positions as fixed contributions and were not refined. All other nongroup atoms except hydrogens were refined with isotropic thermal parameters. The thermal parameters of several carbon atoms on groups 4 and 8 of dimer B were unusually large so these groups were removed and refinement continued without them. A subsequent difference Fourier map confirmed the original positions and indicated that the peaks belonging to the poorly behaved atoms were rather diffuse and about half the intensity of other carbon atoms. No evidence of disorder of these groups was observed so refinement was continued with these groups as before.

At this point an electron density difference map revealed the presence of an unresolved column of electron density in the area enclosed by the phenyl rings of P(A3), P(A4), P(B2), and P(B4). However attempts to fit this volume to CS_2, CH_2Cl_2 or $(C_2H_5)_2O$ molecules were unsuccessful. Unreasonable geometries and thermal parameters resulted and no significant improvement in the crystallographic residuals was observed. The poorly resolved nature of this electron density probably results in part from the loss of solvent of crystallization which

(Continued on p. 241)

TABLE 2

POSITIONAL AND THERMAL PARAMETERS FOR THE NONGROUP ATOMS OF $[Rh_2Cl_2(CO)(C_2S_4)(DPM)_2]$

Atom	x [a]	y	z	B (Å^2)	Atom	x	y	z	B (Å^2)
Rh(A1)	0.7698(1)	0.14302(8)	0.0195(1)	3.87(5)	P(A3)	0.8667(4)	0.1539(3)	0.1171(4)	4.8(2)
Rh(A2)	0.7819(1)	0.02062(8)	0.0180(1)	4.01(5)	P(A4)	0.8685(4)	0.0216(3)	0.1225(3)	4.5(2)
Rh(B1)	0.3290(1)	0.10029(9)	0.59009(9)	3.97(5)	P(B1)	0.3453(4)	0.2008(3)	0.5887(3)	4.7(2)
Rh(B2)	0.2210(1)	0.09598(9)	0.4676(1)	4.59(5)	P(B2)	0.2180(4)	0.1985(3)	0.4603(4)	5.4(2)
Cl(A1)	0.7146(3)	0.1600(3)	0.0895(3)	5.0(2)	P(B3)	0.3241(3)	−0.0009(3)	0.6054(3)	4.3(2)
Cl(A2)	0.8063(4)	−0.0864(3)	0.0165(4)	6.4(2)	P(B4)	0.2070(4)	−0.0069(3)	0.4692(4)	4.9(2)
Cl(B1)	0.2561(3)	0.1230(3)	0.6428(3)	5.2(2)	O(A1)	0.692(1)	−0.0052(8)	0.0809(9)	6.9(5)
Cl(B2)	0.1468(4)	0.0906(3)	0.3477(4)	6.7(2)	O(B1)	0.118(1)	0.102(1)	0.516(1)	11.1(8)
S(A1)	0.7773(3)	0.2435(3)	0.0019(3)	4.8(2)	C(A1)	0.725(1)	0.010(1)	0.058(1)	4.9(6)
S(A2)	0.8120(5)	0.3064(4)	−0.0927(5)	8.3(2)	C(B1)	0.147(1)	0.102(1)	0.493(1)	5.8(7)
S(A3)	0.8280(4)	0.1809(3)	−0.0820(4)	5.2(2)	C(A2)	0.671(1)	0.081(1)	−0.130(1)	4.8(6)
S(A4)	0.8440(3)	0.0612(3)	−0.0352(3)	4.6(2)	C(A3)	0.874(1)	0.090(1)	0.168(1)	3.7(5)
S(B1)	0.4356(3)	0.0967(3)	0.6763(3)	4.6(1)	C(B2)	0.266(1)	0.238(1)	0.538(1)	6.3(7)
S(B2)	0.5696(4)	0.0881(4)	0.6794(4)	7.2(2)	C(B3)	0.248(1)	−0.036(1)	0.555(1)	5.0(7)
S(B3)	0.4555(4)	0.0835(3)	0.5558(4)	5.1(2)	C(A4)	0.802(1)	0.247(1)	−0.057(1)	5.1(6)
S(B4)	0.3210(3)	0.0869(3)	0.4536(3)	5.1(2)	C(A5)	0.815(1)	0.128(1)	−0.033(1)	4.8(6)
P(A1)	0.6671(3)	0.1355(3)	−0.0715(3)	4.3(1)	C(B4)	0.488(1)	0.089(1)	0.639(1)	5.1(6)
P(A2)	0.7000(3)	0.0106(3)	−0.0893(3)	4.0(1)	C(B5)	0.370(1)	0.090(1)	0.530(1)	3.9(5)

[a] Estimated standard deviations in the least significant figure(s) are given in parentheses in this and all subsequent tables.

TABLE 3

DERIVED PARAMETERS FOR THE RIGID GROUP ATOMS OF $[Rh_2Cl_2(CO)(C_2S_4)(DPM)_2]$

Atom	x	y	z	B (Å^2)	Atom	x	y	z	B (Å^2)
C(A11)	0.6397(9)	0.2018(7)	−0.121(1)	3.8(5)	C(B11)	0.3668(8)	0.2406(8)	0.6641(8)	3.9(5)
C(A12)	0.6368(9)	0.2078(7)	−0.1830(9)	6.5(7)	C(B12)	0.3829(9)	0.2129(6)	0.723(1)	5.8(6)
C(A13)	0.610(1)	0.2583(9)	−0.2187(7)	7.7(8)	C(B13)	0.4025(8)	0.2458(8)	0.7796(7)	6.2(7)
C(A14)	0.5863(9)	0.3028(7)	−0.193(1)	7.2(8)	C(B14)	0.4061(8)	0.3066(8)	0.7769(8)	5.4(6)
C(A15)	0.5893(9)	0.2968(7)	−0.1308(9)	7.2(8)	C(B15)	0.3900(9)	0.3343(6)	0.718(1)	9.0(10)
C(A16)	0.616(1)	0.2463(9)	−0.0950(7)	4.5(6)	C(B16)	0.3704(8)	0.3013(8)	0.6614(7)	6.3(7)
C(A21)	0.588(2)	0.1136(8)	−0.0708(7)	4.0(5)	C(B21)	0.410(2)	0.2248(8)	0.565(4)	4.0(5)
C(A22)	0.588(2)	0.0889(8)	−0.015(2)	5.3(6)	C(B22)	0.398(4)	0.2306(8)	0.500(2)	6.4(7)
C(A23)	0.528(2)	0.0718(8)	−0.015(2)	6.7(7)	C(B23)	0.449(5)	0.2448(8)	0.484(3)	4.6(6)
C(A24)	0.469(2)	0.0796(8)	−0.0694(7)	6.4(7)	C(B24)	0.513(2)	0.2532(8)	0.532(4)	6.9(7)
C(A25)	0.469(2)	0.1044(8)	−0.125(2)	7.4(8)	C(B25)	0.525(4)	0.2474(8)	0.597(2)	7.7(8)
C(A26)	0.529(2)	0.1214(8)	−0.126(2)	5.3(6)	C(B26)	0.474(5)	0.2333(8)	0.613(3)	5.4(6)
C(A31)	0.6252(8)	−0.0308(7)	−0.1009(6)	3.1(5)	C(B31)	0.2399(9)	0.2366(8)	0.4029(7)	4.6(6)
C(A32)	0.564(1)	−0.0189(7)	−0.1520(9)	5.2(6)	C(B32)	0.2493(9)	0.2969(8)	0.4077(7)	5.8(7)
C(A33)	0.5088(7)	−0.0519(8)	−0.1599(8)	5.2(6)	C(B33)	0.2667(9)	0.3264(6)	0.3639(9)	8.0(9)
C(A34)	0.5145(8)	−0.0969(7)	−0.1167(6)	5.8(6)	C(B34)	0.2748(9)	0.2954(8)	0.3152(7)	6.7(7)
C(A35)	0.576(1)	−0.1088(7)	−0.0656(9)	5.6(6)	C(B35)	0.2655(9)	0.2350(8)	0.3104(7)	5.8(7)
C(A36)	0.6309(7)	−0.0758(8)	−0.0577(8)	4.8(6)	C(B36)	0.2480(9)	0.2056(6)	0.3543(9)	6.0(7)
C(A41)	0.722(2)	−0.0271(10)	−0.150(2)	4.7(6)	C(B41)	0.136(1)	0.234(1)	0.437(1)	8.2(9)
C(A42)	0.681(1)	−0.0211(9)	−0.215(2)	8.7(9)	C(B42)	0.086(2)	0.220(1)	0.376(2)	10(1)
C(A43)	0.700(3)	−0.045(1)	−0.2610(9)	9(1)	C(B43)	0.024(2)	0.246(2)	0.355(2)	18(2)
C(A44)	0.759(2)	−0.0755(10)	−0.241(2)	6.8(7)	C(B44)	0.012(1)	0.286(1)	0.394(1)	13(1)
C(A45)	0.800(1)	−0.0816(9)	−0.175(2)	11(1)	C(B45)	0.061(2)	0.300(1)	0.455(2)	20(2)
C(A46)	0.782(3)	−0.057(1)	−0.1296(9)	8.6(9)	C(B46)	0.123(2)	0.273(2)	0.477(2)	17(2)
C(A51)	0.863(1)	0.2179(9)	0.167(1)	6.2(7)	C(B51)	0.3300(9)	−0.0263(8)	0.6843(7)	4.1(5)
C(A52)	0.887(1)	0.273(1)	0.1623(8)	8.7(9)	C(B52)	0.3402(8)	0.0128(5)	0.7345(9)	4.9(6)
C(A53)	0.888(1)	0.3177(8)	0.204(1)	10(1)	C(B53)	0.3381(8)	−0.0068(7)	0.7913(7)	6.6(8)
C(A54)	0.865(1)	0.3071(9)	0.251(6)	7.2(8)	C(B54)	0.3257(9)	−0.0656(8)	0.7980(7)	5.4(6)
C(A55)	0.841(1)	0.252(1)	0.2563(8)	9(1)	C(B55)	0.3154(8)	−0.1047(5)	0.7478(9)	5.0(6)
C(A56)	0.840(1)	0.2073(8)	0.214(1)	7.7(9)	C(B56)	0.3176(8)	−0.0851(7)	0.6910(7)	5.3(6)
C(A61)	0.953(2)	0.169(1)	0.128(1)	7.0(8)	C(B61)	0.392(1)	−0.0413(8)	0.598(2)	5.2(6)
C(A62)	1.006(3)	0.165(1)	0.189(3)	7.0(8)	C(B62)	0.451(2)	−0.0459(8)	0.653(2)	4.9(6)
C(A63)	1.069(2)	0.182(1)	0.197(2)	8.5(9)	C(B63)	0.508(1)	−0.0669(8)	0.6481(8)	6.4(7)
C(A64)	1.078(2)	0.203(1)	0.144(1)	15(2)	C(B64)	0.504(1)	−0.0833(8)	0.588(2)	7.4(8)
C(A65)	1.025(3)	0.208(1)	0.084(3)	17(2)	C(B65)	0.445(2)	−0.0788(8)	0.533(2)	4.4(6)
C(A66)	0.962(2)	0.191(1)	0.076(2)	14(2)	C(B66)	0.388(1)	−0.0578(8)	0.5378(8)	5.0(6)
C(A71)	0.8633(9)	−0.0342(7)	0.1789(9)	4.6(6)	C(B71)	0.2354(9)	−0.0541(7)	0.4220(8)	5.4(6)
C(A72)	0.8947(8)	−0.0881(8)	0.1852(7)	6.7(7)	C(B72)	0.2447(9)	−0.1132(8)	0.4381(7)	5.5(7)

TABLE 3 (continued)

C(A73)	0.8910(9)	−0.1297(6)	0.2281(9)	7.5(8)	C(B73)	0.2663(9)	−0.1511(6)	0.4033(9)	6.7(7)
C(A74)	0.8559(9)	−0.1175(7)	0.2646(9)	6.2(7)	C(B74)	0.2786(9)	−0.1298(7)	0.3523(8)	6.3(7)
C(A75)	0.8245(8)	−0.0636(8)	0.2582(7)	5.6(6)	C(B75)	0.2693(9)	−0.0707(8)	0.3362(7)	6.2(7)
C(A76)	0.8282(9)	−0.0220(6)	0.2153(9)	5.1(6)	C(B76)	0.2477(9)	−0.0329(6)	0.3710(9)	4.2(6)
C(A81)	0.953(2)	0.0074(9)	0.1296(7)	4.8(6)	C(B81)	0.123(1)	−0.033(1)	0.447(4)	6.0(7)
C(A82)	0.962(3)	−0.0184(9)	0.079(2)	5.2(6)	C(B82)	0.082(4)	−0.034(1)	0.380(5)	9(1)
C(A83)	1.025(2)	−0.0359(8)	0.088(2)	4.8(6)	C(B83)	0.017(4)	−0.053(1)	0.358(2)	13(1)
C(A84)	1.079(2)	−0.0277(9)	0.1477(7)	7.5(8)	C(B84)	−0.009(1)	−0.070(1)	0.401(4)	14(2)
C(A85)	1.070(3)	−0.0019(9)	0.198(2)	7.8(9)	C(B85)	0.032(4)	−0.069(1)	0.467(5)	20(2)
C(A86)	1.007(2)	0.0157(8)	0.189(2)	6.0(7)	C(B86)	0.097(4)	−0.051(1)	0.490(2)	23(3)

RIGID GROUP PARAMETERS

	x_c [a]	y_c	z_c	Delta [b]	Epsilon	Eta
Ring 1	0.6130(5)	0.2523(6)	−0.1569(6)	−0.44(1)	1.57(1)	4.30(1)
Ring 2	0.5287(6)	0.0966(5)	−0.0701(6)	1.14(1)	2.90(3)	2.40(3)
Ring 3	0.5698(6)	−0.0638(5)	−0.1088(5)	3.84(1)	2.87(1)	3.93(1)
Ring 4	0.7405(7)	−0.0513(6)	−0.1953(8)	2.12(1)	2.05(2)	4.00(3)
Ring 5	0.8642(6)	0.2625(7)	0.2093(7)	0.28(1)	1.28(1)	5.42(2)
Ring 6	1.0155(9)	0.1862(7)	0.1362(9)	4.33(2)	2.66(4)	0.84(4)
Ring 7	0.8596(5)	−0.0759(5)	0.2217(6)	2.76(1)	1.11(1)	5.45(3)
Ring 8	1.0159(6)	−0.0101(5)	0.1387(6)	2.02(1)	2.76(3)	5.55(3)
Ring 9	0.3865(5)	0.2736(6)	0.7205(6)	3.21(1)	1.87(1)	0.57(1)
Ring 10	0.4614(6)	0.2390(5)	0.5486(6)	1.33(1)	2.16(5)	4.60(5)
Ring 11	0.2574(5)	0.2660(6)	0.3591(6)	3.28(1)	1.35(1)	2.63(1)
Ring 12	0.074(1)	0.2600(8)	0.416(1)	−0.84(2)	2.65(3)	3.85(3)
Ring 13	0.3278(5)	−0.0459(5)	0.7412(6)	0.19(1)	1.60(1)	0.33(1)
Ring 14	0.4480(6)	−0.0623(5)	0.5929(6)	−1.20(1)	2.43(3)	1.25(3)
Ring 15	0.2570(5)	−0.0920(5)	0.3872(6)	−0.19(1)	1.31(1)	2.46(1)
Ring 16	0.0570(9)	−0.0516(8)	0.424(1)	4.37(2)	2.15(6)	4.24(6)

[a] x_c, y_c and z_c are the fractional coordinates of the centroid of the rigid group. [b] The rigid group orientation angles Delta, Epsilon and Eta (radians) are the angles by which the rigid body is rotated with respect to a set of axes X, Y and Z. The origin is the centre of the ring: X is parallel to a^*, Z is parallel to c and Y is parallel to the line defined by the intersection of the plane containing a^* and b^* with the plane containing b and c.

TABLE 4

SELECTED DISTANCES (Å) IN $[Rh_2Cl_2(CO)(C_2S_4)(DPM)_2]$

	Dimer A	Dimer B
Bond distances		
Rh(1)—Rh(2)	2.811(3)	2.810(3)
Rh(1)—Cl(1)	2.428(6)	2.455(6)
Rh(2)—Cl(2)	2.508(8)	2.527(8)
Rh(1)—P(1)	2.353(7)	2.327(7)
Rh(2)—P(2)	2.362(7)	2.347(8)
Rh(1)—P(3)	2.367(8)	2.347(7)
Rh(2)—P(4)	2.344(8)	2.372(7)
Rh(1)—S(1)	2.347(7)	2.356(7)
Rh(1)—C(5)	1.90(2)	1.95(2)
Rh(2)—S(4)	2.386(7)	2.393(7)
Rh(2)—C(1)	1.87(2)	1.96(3)
S(1)—C(4)	1.66(2)	1.73(2)
S(2)—C(4)	1.64(3)	1.65(3)
S(3)—C(4)	1.80(3)	1.73(3)
S(3)—C(5)	1.75(3)	1.75(2)
S(4)—C(5)	1.67(3)	1.62(2)
C(1)—O(1)	1.13(2)	1.01(3)
P(1)—C(2)	1.86(2)	1.86(3)
P(2)—C(2)	1.84(3)	1.86(3)
P(3)—C(3)	1.84(2)	1.79(3)
P(4)—C(3)	1.85(2)	1.89(3)
P(1)—C(11)	1.83(1)	1.82(1)
P(1)—C(21)	1.83(1)	1.82(1)
P(2)—C(31)	1.84(1)	1.80(1)
P(2)—C(41)	1.86(2)	1.86(2)
P(3)—C(51)	1.88(2)	1.85(1)
P(3)—C(61)	1.85(2)	1.84(1)
P(4)—C(71)	1.85(1)	1.82(1)
P(4)—C(81)	1.85(1)	1.83(2)
Nonbonded contacts		
P(A1)···P(A2)	3.016(9)	
P(B1)···P(B2)	3.094(11)	
P(A3)···P(A4)	3.025(10)	
P(B3)···P(B4)	3.096(10)	
Cl(A2)···H(A46)	2.42	
Cl(B2)···H(B42)	2.61	
O(A1)···H(A22)	2.53	
H(A76)···H(A3)	2.08	
H(A86)···H(A4)	2.16	
H(A13)···H(B25) [a]	2.27	
H(A65)···H(B45) [b]	2.09	

[a] Atom located at x, y, $-1 + z$. [b] Atom located at $1 + x$, $1/2 - y$, $-1/2 + z$.

was observed during data collection (vide supra) and explains the poor diffraction quality of the crystals and the decrease in intensities of the standard reflections during data collection.

The final model with 337 parameters varied converged to $R = 0.114$ and $R_w = 0.145$ [24]. At this point an electron density difference map showed the highest 20 peaks (2.69—1.00 $e/Å^3$) were in the vicinities of the heavy atoms

TABLE 5

SELECTED ANGLES (deg) IN $[Rh_2Cl_2(CO)(C_2S_4)(DPM)_2]$

	Dimer A	Dimer B
Rh(2)—Rh(1)—S(1)	162.9(2)	164.3(2)
Rh(2)—Rh(1)—Cl(1)	104.2(2)	91.7(2)
Rh(2)—Rh(1)—C(5)	74.7(8)	76.0(7)
Rh(2)—Rh(1)—P(1)	88.8(2)	95.4(2)
Rh(2)—Rh(1)—P(3)	93.5(2)	92.2(2)
Rh(1)—Rh(2)—Cl(2)	172.9(2)	165.5(2)
Rh(1)—Rh(2)—S(4)	72.5(2)	71.5(2)
Rh(1)—Rh(2)—C(1)	91.8(8)	100.3(8)
Rh(1)—Rh(2)—P(2)	94.1(2)	91.3(2)
Rh(1)—Rh(2)—P(4)	91.2(2)	94.7(2)
Cl(1)—Rh(1)—S(1)	92.9(2)	104.0(2)
Cl(1)—Rh(1)—C(5)	178.1(8)	166.5(7)
Cl(1)—Rh(1)—P(1)	91.0(2)	86.5(2)
Cl(1)—Rh(1)—P(3)	83.1(2)	93.0(2)
Cl(2)—Rh(2)—S(4)	101.2(2)	93.9(2)
Cl(2)—Rh(2)—C(1)	94.5(8)	94.3(9)
Cl(2)—Rh(2)—P(2)	88.2(2)	89.2(3)
Cl(2)—Rh(2)—P(4)	86.2(3)	86.5(3)
S(1)—Rh(1)—C(5)	88.2(8)	88.5(7)
S(1)—Rh(1)—P(1)	92.0(3)	86.4(3)
S(1)—Rh(1)—P(3)	87.4(3)	86.3(2)
S(4)—Rh(2)—C(1)	164.1(8)	171.7(9)
S(4)—Rh(2)—P(2)	82.5(2)	94.4(3)
S(4)—Rh(2)—P(4)	96.2(2)	93.0(2)
C(5)—Rh(1)—P(1)	90.6(8)	89.3(7)
C(5)—Rh(1)—P(3)	95.4(8)	92.9(7)
C(1)—Rh(2)—P(2)	96.5(8)	87.0(8)
C(1)—Rh(2)—P(4)	86.4(8)	86.2(8)
P(1)—Rh(1)—P(3)	174.0(2)	172.3(3)
P(2)—Rh(2)—P(4)	173.9(3)	171.6(3)
Rh(1)—S(1)—C(4)	105.2(9)	104.4(9)
S(1)—C(4)—S(2)	127(2)	123(2)
S(1)—C(4)—S(3)	118(2)	119(2)
S(2)—C(4)—S(3)	114(1)	118(1)
C(4)—S(3)—C(5)	102(1)	104(1)
Rh(1)—C(5)—S(3)	124(1)	123(1)
Rh(1)—C(5)—S(4)	120(1)	117(1)
S(3)—C(5)—S(4)	116(1)	119(1)
Rh(2)—S(4)—C(5)	91.4(8)	95.0(8)
Rh(2)—C(1)—O(1)	169(2)	166(3)
Rh(1)—P(1)—C(2)	111.1(8)	110.4(9)
Rh(2)—P(2)—C(2)	113.3(9)	115(1)
Rh(1)—P(3)—C(3)	108.4(8)	116.2(9)
Rh(2)—P(4)—C(3)	114.4(8)	111.1(9)
Rh(1)—P(1)—C(11)	115.3(6)	117.4(7)
Rh(1)—P(1)—C(21)	126.0(7)	116.7(6)
Rh(2)—P(2)—C(31)	116.9(6)	121.6(7)
Rh(2)—P(2)—C(41)	118.8(8)	116(1)
Rh(1)—P(3)—C(51)	113.4(7)	117.8(6)
Rh(1)—P(3)—C(61)	129(1)	121.9(6)
Rh(2)—P(4)—C(71)	115.6(6)	119.8(7)
Rh(2)—P(4)—C(81)	117.1(7)	116.6(8)
P(1)—C(2)—P(2)	109(1)	113(1)
P(3)—C(3)—P(4)	110(1)	115(1)
C(2)—P(1)—C(11)	102(1)	99(1)
C(2)—P(1)—C(21)	99(1)	110(1)
C(2)—P(2)—C(31)	106(1)	103(1)
C(2)—P(2)—C(41)	100(1)	99(2)

TABLE 5 (continued)

	Dimer A	Dimer B
C(3)—P(3)—C(51)	105(1)	98(1)
C(3)—P(3)—C(61)	105(1)	107(1)
C(3)—P(4)—C(71)	101.2(9)	105(1)
C(3)—P(4)—C(81)	106(1)	99(1)
C(11)—P(1)—C(21)	99.4(8)	101.8(8)
C(31)—P(2)—C(41)	99.5(8)	97(1)
C(51)—P(3)—C(61)	94(1)	102.4(8)
C(71)—P(4)—C(81)	100.5(9)	102(1)

and the column of electron density. A typical carbon atom on an earlier synthesis had an electron density of 3.2 $e/Å^3$. The high crystallographic residuals result from the poor diffraction quality of the crystal, the unaccounted for column of electron density in the lattice, which is due presumably to solvent of crystallization which was lost during data collection (vide supra) and the isotropic refinement of the model. An anisotropic refinement, of at least the heavy atoms (Rh, Cl, S and P), would have been desirable since much of the residual electron density lies in the regions near these atoms. However, this was not attempted due to the extremely high cost associated with such a refinement. In spite of the high R factors however, there is no ambiguity about the correctness of the structure. Both independent dimers are very similar with good agreement in their parameters, all of which are chemically reasonable (vide infra). Where differences in the two dimers show up these differences are readily explained based on the non-bonded contacts in the cell (vide infra).

The positional and thermal parameters for the individual isotropic atoms and rigid group atoms are given in Tables 2 and 3, respectively. Selected bond lengths and angles are shown in Tables 4 and 5, respectively. A listing of observed and calculated structure amplitudes and tables of least-squares plane calculations, torsion angles and the idealized hydrogen atom parameters are available *.

Discussion

Description of structure

Figure 1 shows the two dimers and their numbering schemes and Figure 2 presents the atoms in the equatorial planes together with some relevant distances.

The complex, $[Rh_2Cl_2(CO)(C_2S_4)(DPM)_2]$ (3), crystallizes with two independent molecules per asymmetric unit. Both dimers have the same overall geometry, as shown in Fig. 1, with the Rh centers bridged by two transoid DPM ligands, but differ slightly in the orientations of the ligands (vide infra). Within

* See NAPS document no. 03822 for 22 pages of supplementary material. Order from NAPS c/o Microfiche Publications, P.O. Box 3513, Grand Central Station, New York, N.Y. 10017. Remit in advance, in U.S. funds only, $ 5.50 for photocopies or $ 3.00 for microfiche. Outside the U.S. and Canada add postage of $ 3.00 for photocopy and $ 1.00 for microfiche.

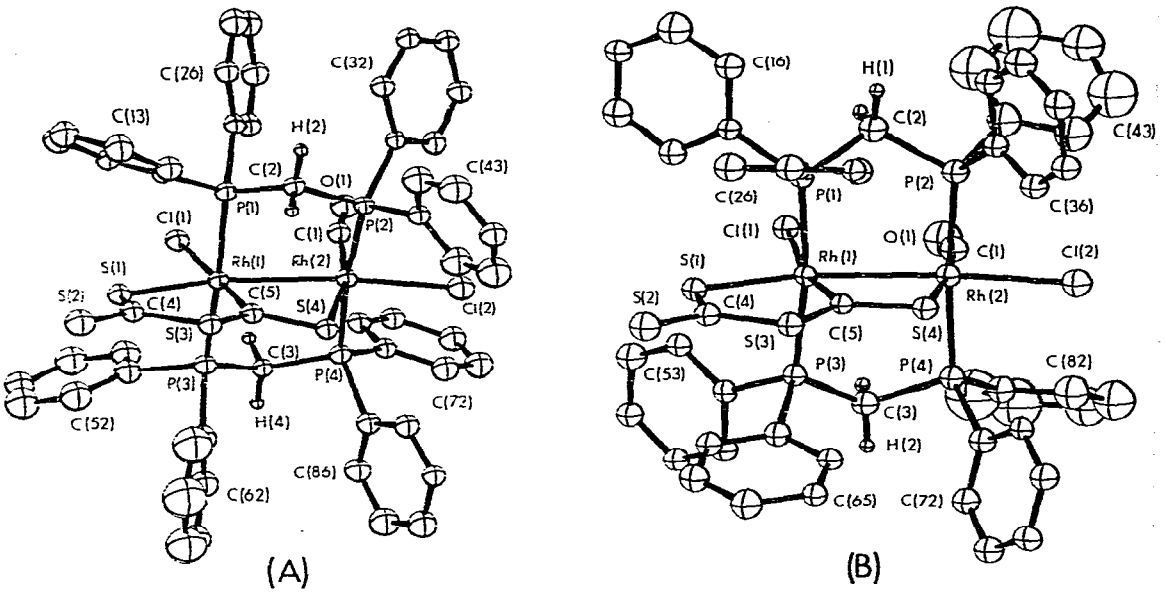

Fig. 1. A perspective view for dimers A and B of $[Rh_2Cl_2(CO)(C_2S_4)(DPM)_2]$ showing the numbering scheme used.

each dimer the Rh atoms display distorted octahedral coordinations. One rhodium atom of each dimer (Rh(Al), Rh(B1)) * has two mutually *trans* P atoms in the axial sites with the equatorial positions occupied by a sulfur and a carbon atom of the C_2S_4 fragment, a chloro ligand and the other Rh atom. The second Rh atom (Rh(A2), Rh(B2)) also has mutually *trans*, axial P atoms, with a sulfur atom of the C_2S_4 moiety, a chloro ligand, a carbonyl group and the other Rh atom occupying its equatorial sites.

The Rh—Rh distances of 2.811(3) Å and 2.810(3) Å, for dimers A and B, respectively, compare well with each other and are consistent with a normal Rh—Rh single bond, falling within the range previously reported for such distances in similar complexes (2.7447(9) to 2.8145(7) Å) [25—28]. As is typically observed when metal—metal bonding is involved in these DPM-bridged dimers, the Rh—Rh distance is significantly shorter than the intraligand P—P distances (see Table 4). This can be seen clearly in Fig. 1 where the compression of the Rh—Rh vector is evident.

The Rh—C and C—O distances of the carbonyl ligands are not unusual, comparing acceptably with other determinations [25,29—31]. However, both carbonyl groups are significantly bent (Rh(A2)—C(A1)—O(A1) = 169(2)°, Rh(B2)—C(B1)—O(B1) = 166(3)°). A consideration of the nonbonded contacts indicates that in both dimers the carbonyl ligands bend in such a way as to minimize the contacts with the phenyl rings suggesting that the bending of these ligands is steric in origin.

The rhodium—chlorine distances (Rh(A1)—Cl(A1) = 2.428(6) Å; Rh(B1)—Cl(B1) = 2.455(6) Å) which are *trans* to C(A5) and C(B5), respectively, are

* Rh(A1) refers to atom Rh(1) of dimer A.

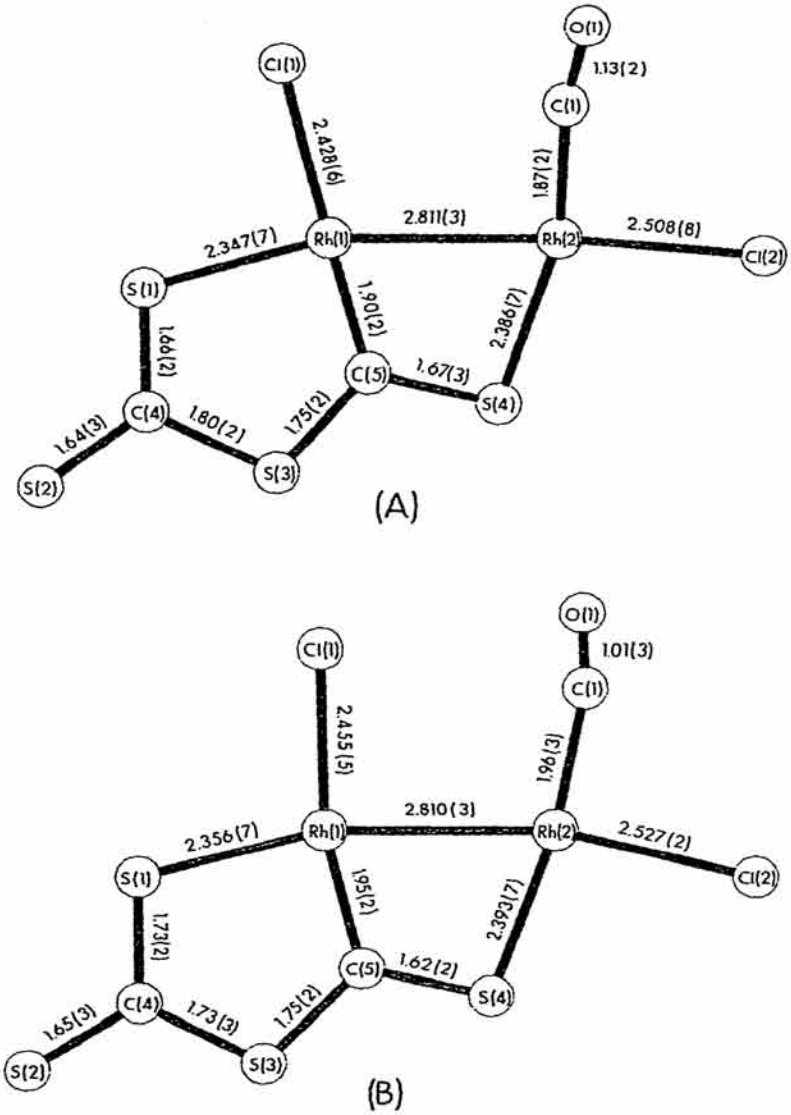

Fig. 2. Views of the equatorial planes of dimers A and B showing some relevant bond distances.

quite long but compare well with other determinations, where the chloro ligand is *trans* to a σ-bound alkenyl group or carbene ligand [15,16,32]. On the other hand, the Rh(2)—Cl(2) bond distances (2.508(8) Å and 2.527(8) Å for molecules A and B, respectively), which are opposite the rhodium atoms, Rh(A1) and Rh(B1), are significantly longer than those typically observed in these systems [26,28,30,31]; in fact they are even longer than those observed when a chloro ligand is opposite a ligand of high *trans* influence such as a carbene and suggest that these chloro ligands may be loosely coordinated (vide infra). These long rhodium—chloro distances, we suspect, arise as a result of steric crowding about the Rh(2) center. Support for this comes from the short nonbonded

phenyl hydrogen—chloro contacts observed for these two chloro ligands (Cl(A2)—H(A46) = 2.42 Å; Cl(B2)—H(B42) = 2.61 Å). Furthermore, these interactions are such that they tend to force these chloro ligands away from the metal centers (see Fig. 1).

The C_2S_4 fragment contains two intact CS_2 molecules (S(1)C(4)S(2) and S(3)C(5)S(4) fused at C(4)—S(3). This fragment is then bound to one rhodium atom (Rh(1)) via S(1) and C(5) and to the other rhodium atom through S(4). Within the resulting $Rh_2C_2S_4$ metallocycles the C—S distances (1.64(3)—1.80(3) Å, dimer A; 1.65(3)—1.75(2) Å, dimer B) and angles (see Table 5) compare favourably with those reported for $[Rh(\eta^5\text{-}C_5H_5)(C_2S_4)(PMe_3)]$ [9], where an analogous C_2S_4 fragment was observed. These distances suggest delocalization over the carbon—sulfur framework and range from values comparable to the C—S double bond distance observed in ethylene thiourea (1.71 Å) [33] to single bond values (1.81 Å) [33]. The Rh(1)—S(1) and Rh(2)—S(4) distances (average 2.352(7) and 2.390(7) Å, respectively), although significantly different, compare favourably with other determinations involving Rh—S bonds [15,16,34,35].

The C_2S_4 ligand can be considered as a carbene ligand, $C_2S_4^{2-}$, with each of the coordinated sulfur atoms and the carbene atom functioning as two electron donors to the rhodium atoms, as shown below in the valence bond formulation. Therefore the rhodium atoms are formally Rh^{II}. The usually short Rh(1)—C(5)

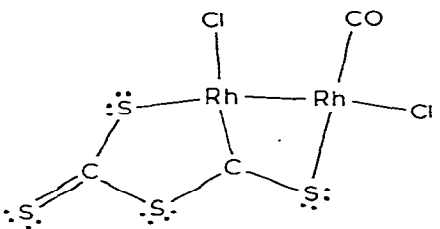

distances (1.90(2) and 1.95(2) Å, for dimers A and B, respectively) are comparable to the rhodium carbonyl distances, suggesting significantly multiple bond character. They are also comparable to other such distances and are especially close to those observed in $[RhCl(PPh_3)_2(PhCONCS)_2]$ [15] and $[RhCl(PPh_3)_2(EtOCONCS)_3]$ [16], in which rather analogous five-membered metallocycle rings again resulted as a consequence of condensation of sulfur-containing molecules on rhodium. This distance also compares well with the value of 1.95(1) Å, observed in the iridium complex, $IrCl(C_2O_4)(PMe_3)_3$, which contains an analogous C_2O_4 fragment [11]. The short Rh—C distances in these rhodium and iridium metallocycles may result from π bonding between the carbene carbon atoms and the metal atoms or may be a consequence of the rest of the metallocycle forcing the central carbon atoms close to the metal atoms. In $[Rh(\eta^5\text{-}C_5H_5)(C_2S_4)(PMe_3)]$ the analogous Rh—C distance (2.04(1) Å) is somewhat longer than observed here although it is still short [9].

Within the DPM framework the parameters are, on the whole, not unusual and compare well with other determinations [25—31]; the Rh—P and P—C distances and the angles within the DPM framework are all typical for DPM-bridged rhodium dimers. It is noteworthy, however, that the two independent dimers in this structure do differ significantly in the orientations of the DPM ligands. One obvious difference lies in the orientations of the bridging methyl-

ene groups of the DPM ligands; in dimer A these CH_2 groups are *trans* whereas they are *cis* in dimer B. In general when the environments on each side of the rhodium—phosphine plane are not identical a *cis*-methylene arrangement is found [25—29]. However, in these cases the methylene groups usually bend towards the more crowded side of the molecule, minimizing non-bonded contacts with the bulky phenyl rings. In dimer B the methylene groups are bent away from the bulky C_2S_4 group, thereby thrusting four phenyl groups into the vicinity of the C_2S_4 group. To minimize contacts with this equatorial ligand, two of the phenyl rings orient themselves almost parallel to it while the other two are nearly perpendicular to the C_2S_4 plane but aimed between the S(4) and Cl(2) atoms. This arrangement of the phenyl groups results in an almost planar C_2S_4 group giving the molecule approximate C_s symmetry through the equatorial plane. In contrast, the C_2S_4 group in dimer A is significantly puckered owing to the vastly different phenyl group orientations compared to dimer B; in particular ring 6 in dimer A is perpendicular to the C_2S_4 plane instead of parallel to it, as in B.

The two dimers also differ in the degree of twist about the metal—metal bond; dimer A is severely twisted whereas dimer B has a relatively planar rhodium phosphine framework (see Fig. 1). In dimer B, apart from the two rings which are parallel to the C_2S_4 ligand, all phenyl groups aim between the equatorial ligand positions avoiding unfavourable nonbonded contacts. However, in dimer A the phosphine framework twists to avoid unfavourable contacts between ring 3 and the carbonyl group. If no twisting had occurred these groups would be in an unfavourable eclipsed conformation.

The above differences in the phenyl ring orientations also lead to differences in the equatorial ligand orientations. As already noted, one such result is the puckering of the C_2S_4 moiety in dimer A. In addition, the orientations of the chloro and carbonyl ligands differ in the two dimers (this is seen clearly in Fig. 2). These groups tend to stagger themselves with respect to the phenyl groups. For example in Fig. 1 we see that for dimer A, ring 2 falls between Cl(1) and Rh(2), forcing Cl(1) towards S(1), whereas in dimer B phenyl ring 1 falls between S(1) and Cl(1), forcing Cl(1) in this dimer towards Rh(2). Similarly the bending of the carbonyl ligands in opposite directions also results from different phenyl ring contacts. Therefore the differences observed in the two dimers can be seen to be steric in origin. A consideration of intermolecular contacts shows that there are no unusual interactions which would readily account for the above differences in the dimers.

Reactions of trans-[RhCl(CO)(DPM)]$_2$ and [Rh$_2$Cl$_2$(μ-CO)(DPM)$_2$] with CS$_2$

The reaction of either *trans*-[RhCl(CO)(DPM)]$_2$ (1) or [Rh$_2$Cl$_2$(μ-CO)-(DPM)$_2$] (2) with CS_2 results in the formation of the final product, [Rh$_2$Cl$_2$(CO)(C_2S_4)(DPM)$_2$] (3). A detailed spectroscopic study ($^{31}P\{^1H\}$ and $^{13}C\{^{31}P\{^1H\}\}$ NMR and infrared, using ^{13}CO enriched [Rh$_2$Cl$_2$(μ-^{13}CO)(DPM)$_2$] for the ^{13}C NMR experiments) of the stepwise addition of CS_2 to a solution of 2 yields much valuable information regarding the intermediates in the reaction. However, we should caution that Scheme 1, showing the postulated reaction sequence, is still somewhat speculative and represents what we feel is the most probable sequence based on the evidence and on our experience with analogous

SCHEME 1

THE REACTION OF $[Rh_2Cl_2(\mu\text{-CO})(DPM)_2]$ (2) WITH CS_2

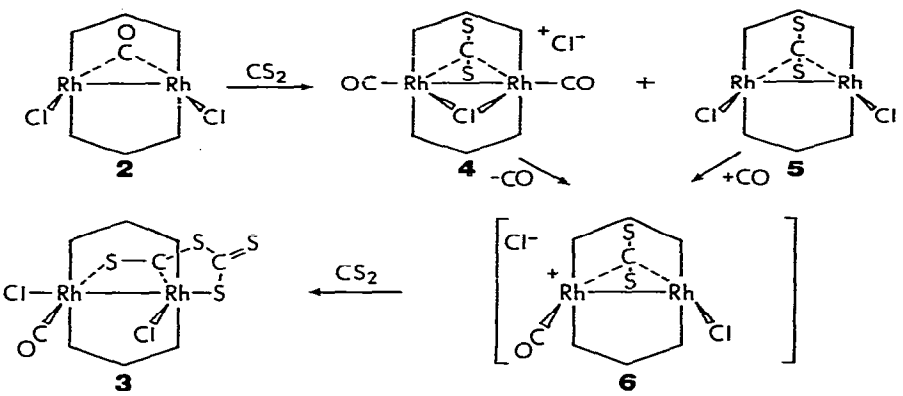

systems [25—27,30]. Initially, in the $^{31}P\{^1H\}$ NMR spectrum resonances assignable to unreacted 2 and two other symmetric species (4 and 5, Scheme 1) are observed. Species 4 is believed to be a dicarbonyl species because of the close similarity of its ^{31}P NMR spectrum with those of the well characterized SO_2 [26] and CO [25] analogues, $[Rh_2(CO)_2(\mu\text{-Cl})(\mu\text{-}SO_2)(DPM_2]^+$ and $[Rh_2(CO)_2(\mu\text{-Cl})(\mu\text{-CO})(DPM)_2]^+$, respectively, and because of the simultaneous appearance in the infrared spectrum of one new vibration in the terminal carbonyl region at 1990 cm^{-1}. The resonance due to 5 is similar to those of the analogous monocarbonyl species, 2, and the SO_2 analogue, $[Rh_2Cl_2(\mu\text{-}SO_2)(DPM)_2]$ [26] and is therefore assigned a similar structure to these species as shown in Scheme 1. Species 4 and 5 result from CO transfer during the reaction of 2 with CS_2 as has previously been observed in the analogous reaction of 2 with SO_2 [30] where facile carbonyl transfer was also observed, yielding di- and tricarbonyl, as well as carbonyl-free products at intermediate times. What the actual sequence of events yielding these species is, or what other intermediates might be involved in their formation is not known. As one referee suggested, rather than proceeding directly as indicated in the scheme, CS_2 attack on 2 might yield 5 with the liberated CO reacting with 2 giving the dichlorodicarbonyl species 1 which subsequently reacts with CS_2 to give 4 (see Scheme 2). However, we have no evidence to support or refute this or any other reaction sequence; we know only that 4 and 5 appear essentially simultaneously.

Soon after the appearance of 4 and 5 the resonance due to the final species, 3, is observed. This resonance in the $^{31}P\{^1H\}$ NMR spectrum appears as a complex multiplet at δ = 7.5 ppm arising from the AA'BB'XY spin system. Again, how species 4 and 5 give rise to the final product is a matter of speculation since no other resonance is clearly definable in the $^{31}P\{^1H\}$ NMR spectra. But based on our previous studies and on the fact that both 4 and 5 eventually yield the same monocarbonyl species, 3, we feel that 6 is a reasonable intermediate. If CO loss from 4 occurs, 6 would simply result from the Cl atom swinging out of the bridging position into the vacated site. Just such a transformation has been observed for the bromocarbonyl analogue of 4, $[Rh_2(CO)_2(\mu\text{-Br})(\mu\text{-CO})(DPM)_2]^+ Br^-$, in which carbonyl loss yields $[Rh_2Br(CO)(\mu\text{-CO})$-

SCHEME 2

THE REACTION OF *trans*-[RhCl(CO)(DPM)]$_2$ (1) with CS_2

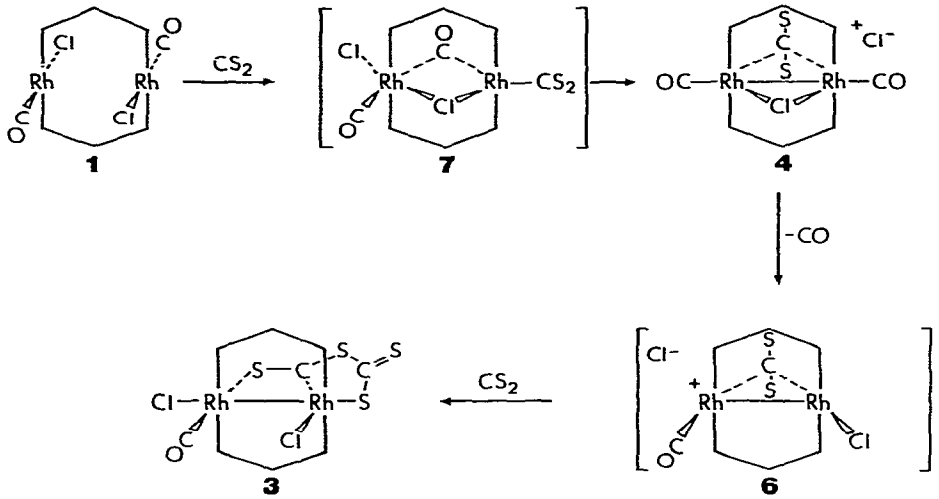

$(DPM)_2]^+ Br^-$, an asymmetric species analogous to 6 [30]. Furthermore, if CO attacks 5 we would expect it to attack between the CS_2 and Cl ligands yielding 6. Again there is a precedent in the reaction of $[Rh_2Br_2(\mu\text{-CO})(DPM)_2]$ with CO, which also yields $[Rh_2Br(CO)(\mu\text{-CO})(DPM)_2]^+ Br^-$ [30].

Electrophilic attack at one of the sulfur atoms of the bound CS_2 molecule by another CS_2 molecule would then readily yield the final product 3 by C—S bond formation (between C(4) and S(3) of Fig. 1), Rh—S bond formation (between Rh(1) and S(1) and between Rh(2) and S(4)) and Rh—C bond rupture (Rh(2)—C(5)). Again it must be reemphasized that we have no direct information regarding any possible species between compounds 4 and 5 and the final product. However, it is encouraging that some ionic intermediate such as 6 is supported by the X-ray study in which the very long Rh(2)—Cl(2) bond length (vide supra) suggests loose coordination of this chloro-ligand. It is also noteworthy that in the absence of excess CS_2 this process is reversible, giving back compound 2. Based on the X-ray determination we would suggest that the first step in this loss of C_2S_4 is chloride ion dissociation.

The ^{13}C NMR spectra of the same reaction using $[Rh_2Cl_2(\mu\text{-}^{13}CO)(DPM)_2]$ initially shows the carbonyl resonance assignable to 2, as well as one additional species at δ = 186.5 ppm (doublet, $|^1J(Rh—C)|$ = 80.1 Hz), characteristic of a terminal carbonyl ligand and consistent with species 4. The $^{31}P\{^1H\}$ NMR spectrum at this stage showed two resonances (due to 2 and 4) split by the ^{13}C nuclei and one resonance (5) unsplit by ^{13}C, indicating that indeed species 5 is free of ^{13}CO. The only other carbonyl resonance observed later in the experiment is assignable to species 3 at δ = 191.5 ppm (doublet, $|J(Rh—C)|$ = 69.1 Hz). Similarly, the infrared spectrum * shows only bands assignable to 2, 3 and

* All infrared results are for ^{12}CO complexes.

a band at 1990 cm^{-1} which is again consistent with species 4. Therefore all the spectral parameters and the analogies with the SO_2 [26,30] and carbonyl [30] chemistry appear to support this scheme.

Since in each of compounds 4 and 5 the four phosphorus atoms are shown in the ^{31}P NMR spectra to be chemically equivalent at —50° C, it is suggested that the CS_2 ligands in these species are coordinated solely through the carbon atoms, as has been proposed for CO_2 in some of its compounds [36,37], and as has been observed in one such complex [12]. The CS_2 groups would therefore lie perpendicular to the Rh—Rh vectors with quasi-tetrahedral geometries of the carbon atoms. A C—S-bound species would give rise to a more complex ^{31}P NMR spectrum owing to the resulting chemical inequivalence of the phosphorus atoms, unless the CS_2 molecule were fluctional at this temperature. No evidence suggesting fluctionality of these species was observed, although we were unable to carry out this study at temperatures lower than —50° C owing to solubility problems.

Based on these studies on the reaction of 2 with CS_2 and on analogies with the previous studies involving CO and SO_2 [30] we can postulate a scheme for the reaction of 1 with CS_2 (see Scheme 2). Initial attack is probably terminal since this is the only site open to attack [30]. The resulting species, $[Rh_2Cl(CO)(CS_2)(\mu\text{-}Cl)(\mu\text{-}CO)(DPM)_2]$ (7), although not observed, is analogous to that proposed, based on spectral data, for the initial species in SO_2 attack on 1 [26]. This species we believe then rearranges to $[Rh_2(CO)_2(\mu\text{-}Cl)(\mu\text{-}CS_2)(DPM)_2][Cl]$ (4), identical to the species observed in the reaction of 2 (Scheme 1). Chloride recoordination and carbonyl loss would then proceed as proposed in Scheme 1 with subsequent CS_2 attack yielding the final species 3.

Conclusions

This study presents only the second structural characterization of a rhodium-carbon disulfide complex and is the first such binuclear species. It is notable that the only two such complexes characterized in fact contain C_2S_4 fragments resulting from activation of a metal-bound CS_2 molecule and its subsequent condensation with another CS_2 molecule. Based on the similarities in the infrared spectral parameters between these complexes and other species which were believed to contain C,S-η^2 side-on bound CS_2, we suggest that these CS_2 species might instead be C_2S_4 complexes. Certainly it is becoming apparent that rhodium has a tendency for activating and condensing sulfur-containing molecules, as has now been demonstrated by several structural determinations [9,15,16]. In addition, one of the few structurally characterized [11] CO_2 complexes, $[IrCl(C_2O_4)(PPh_3)_3]$, contains an analogous C_2O_4 moiety, indicating the similarities in the chemistry involving CO_2 and CS_2.

Our proposed carbon-bound CS_2 intermediates are especially germane to the CS_2 condensation reaction since electrophilic attack at a sulfur atom of the carbon-bound CS_2 group by a free CS_2 molecule would readily yield the observed C_2S_4 fragment. Although this CS_2 bonding mode is unprecedented in CS_2 chemistry, a carbon-bound CO_2 complex has been characterized [12], and certainly these proposed intermediates fit our spectral data and present logical intermediates in the production of the final species 3.

The detailed spectroscopic investigation of the stepwise addition of CS_2 to the binuclear complex, $[Rh_2Cl_2(\mu\text{-}CO)(DPM)_2]$, is believed to be the first such study and has proven invaluable in obtaining important information regarding the natures of the intermediate species in the reaction and the ligand rearrangements that are possible in binuclear complexes. This spectroscopic study, together with the structural determination of the final product, yields valuable insights into the transition metal activation of CS_2, particularly in complexes of rhodium.

Acknowledgmants

We thank the University of Alberta and the Natural Sciences and Engineering Council of Canada for financial support, and Mr. Tom Brisbane for assistance with the NMR experiments.

References

1 I.S. Butler and A.E. Fenster, J. Organometal. Chem., 66 (1974) 161; and references therein.
2 M. Baird, G. Hartwell, Jr., R. Mason, A.I.M. Rae and G. Wilkinson, Chem. Commun. (1967) 92.
3 J.M. Lisey, E.D. Dobrzynski, R.J. Angelici and J. Clardy, J. Amer. Chem. Soc., 97 (1975) 656.
4 T.G. Southern, D.Sc. Thesis, L'Université de Rennes, 1979.
5 R. Mason and A.I.M. Rae, J. Chem. Soc. A, (1970) 1767.
6 T. Kashiwagi, N. Yasuoka, T. Ueki, N. Kasai, M. Kakuda, S. Takahashi and N. Hagihara, Bull. Chem. Soc. Jap., 41 (1968) 296.
7 H. Werner, K. Leonhard and Ch. Burschka, J. Organometal. Chem., 160 (1978) 291.
8 H. LeBozec, P.H. Dixneuf, A.J. Carty and N.J. Taylor, Inorg. Chem., 17 (1978) 2568.
9 a) H. Werner, O. Kolb, R. Feser and U. Schubert, J. Organometal. Chem., 191 (1980) 283. b) H. Werner, private communication.
10 M. Aresta, C.F. Nobile, V.G. Albano, E. Forni and M. Manassero, J. Chem. Soc., Chem. Commun., (1975) 636.
11 T. Herskovitz and L.J. Guggenberger, J. Amer. Chem. Soc., 98 (1976) 1615.
12 G. Fachinetti, C. Floriani, P.F. Zanazzi, J. Amer. Chem. Soc., 100 (1978) 7405.
13 M.C. Baird and G. Wilkinson, J. Chem. Soc. A, (1967) 865.
14 D. Commereuc, I. Douek and G. Wilkinson, J. Chem. Soc. A, (1970) 1771.
15 a) M. Cowie, J.A. Ibers, Y. Ishii, K. Itoh, I. Matsuda and F. Ueda, J. Amer. Chem. Soc., 97 (1975) 4748. b) M. Cowie and J.A. Ibers, Inorg. Chem., 15 (1976) 552.
16 K. Itoh, I. Matsuda, F. Ueda, Y. Ishii and J.A. Ibers, J. Amer. Chem. Soc., 99 (1978) 2118.
17 The cell reduction was performed using a modification of TRACER II by S.L. Lawson. See: S.L. Lawson, R.A. Jacobson, The Reduced Cell and Its Crystallographic Applications, Ames Laboratory Report IS-1141; USEAC: Iowa State University, Ames, Iowa, April, 1965.
18 R.J. Doedens and J.A. Ibers, Inorg. Chem., 6 (1967) 204.
19 Besides local programs the following were used in the solution and refinement of the structure: FORDAP, the Fourier summation program by A. Zalkin; SFLS-5, structure factor and least-squares refinement by C.J. Prewitt; ORFFE, for calculating bond lengths, angles and associated standard deviations by W. Busing and H.A. Levy; ORTEP, plotting program by C.K. Johnson; AGNOST, the Northwestern University absorption program which includes the Coppens-Leiserowitz-Rabinovich logic for Gaussian integration.
20 G. Germain, P. Main and M.M. Woolfson, Acta Crystallogr. A., 27 (1971) 368.
21 D.T. Cromer and J.T. Waber, International Tables for X-ray Crystallography, The Kynoch Press, Birmingham, England, 1974, Vol. IV, Table 2.2 A.
22 R.F. Stewart, E.R. Davidson and W.T. Simpson, J. Chem. Phys., 42 (1965) 3175.
23 D.T. Cromer and D.J. Liberman, J. Chem. Phys., 53 (1970) 1891.
24 $R = \Sigma \| F_o | - | F_c \| / \Sigma | F_o |$ $R_w = [\Sigma w(|F_o| - |F_c|)^2 / \Sigma w F_o^2]^{1/2}$
25 a) M. Cowie, J. Mague and A.R. Sanger, J. Amer. Chem. Soc., 100 (1978) 2628. b) M. Cowie, Inorg. Chem., 18 (1979) 286.
26 a) M. Cowie, S.K. Dwight and A.R. Sanger, Inorg. Chim. Acta, 31 (1978) L407. b) M. Cowie and S.K. Dwight, Inorg. Chem., 19 (1980) 209.
27 M. Cowie and S.K. Dwight, Inorg. Chem., 19 (1980) 2508.

28 M. Cowie and R.S. Dickson, Inorg. Chem., in press.
29 M. Cowie and S.K. Dwight, Inorg. Chem., 18 (1979) 2700.
30 M. Cowie and S.K. Dwight, Inorg. Chem., 19 (1980) 2500.
31 M. Cowie and S.K. Dwight, Inorg. Chem., in press.
32 B. Cetinkaya, M.F. Lappert, G.M. McLaughlin and K. Turner, J. Chem. Soc. Dalton, (1974) 1591.
33 International Tables for X-ray Crystallography, 3rd Ed., The Kynoch Press, Birmingham, England, Vol. III, 1972, p. 276.
34 R. Beckett and B.F. Hoskins, Inorg. Nuc. Chem. Lett., 8 (1972) 683.
35 V.R. Richter, J. Kaiser, J. Sieler and L. Kutschobsky, Acta Crystallogr. B, 31 (1975) 1642.
36 M. Aresta and C.F. Nobile, J. Chem. Soc. Dalton, (1977) 708.
37 T. Herskovitz, J. Amer. Chem. Soc., 99 (1977) 2391.